Semiconducting spin glass to metallic ferromagnetic state phase transition in double-substituted La$_{1-x}$Sr$_x$Co$_{1-y}$Ni$_y$O$_{3-\gamma}$ perovskites

R. A. Lanovsky [1,*] M. V. Bushinsky,[1] N. V. Tereshko,[1] O. S. Mantytskaya,[1] A. V. Nikitin [1,] and D. P. Kozlenko[2]

[1]*SSPA "Scientific-Practical Materials Research Centre of NAS of Belarus," P. Brovka Street 19, 220072 Minsk, Belarus*
[2]*Frank Laboratory of Neutron Physics, JINR, Dubna, Moscow Region, Russian Federation*

A comprehensive study of the structural, magnetic, and transport properties of double-substituted La$_{1-x}$Sr$_x$Co$_{1-y}$Ni$_y$O$_{3-\gamma}$ ($0.1 \leqslant x \leqslant 0.5$, $0.05 \leqslant y \leqslant 0.25$) perovskite systems was carried out. The average oxidation number of Co ions was found to be 3+ for the most subsystems. The existence of several characteristic concentration regions for various degrees of substitution in the A (La, Sr) and B (Co, Ni) sublattices is shown. Low levels of Sr and Ni ion substitution subsystems demonstrate cluster spin-glass behavior with a semiconducting character of the conductivity and a diamagnetic low-spin (LS) Co^{3+} matrix. An increase of Ni substitution leads to the stabilization of intermediate-spin (IS) Co^{3+} ions in CoO$_6$ octahedra, approaching the percolation threshold of ferromagnetic clusters. For strongly Sr-substituted subsystems an effect of stabilization of IS Co^{3+} is not observed, since the contribution of this effect is smaller than the effect of the dilution by antiferromagnetically interacting Ni ions. In this case, an increase of Ni content leads to a decrease in the magnetic ordering temperature T_{mo} and magnetization values. For weakly Sr-substituted systems, on the contrary, it leads to their growth. Anomalies in the conductivity dependences for several subsystems are due to the thermally induced spin crossover of the part of Co^{3+} ions, first from the LS to the IS state, and then to the mixed IS/high-spin (HS) state, similar to the parent LaCoO$_3$.

I. INTRODUCTION

Complex cobalt oxides with a perovskite-related structure are of considerable research interest, taking into account prospective technological applications and a range of challenging physical phenomena they demonstrate [1,2]. They are promising materials for use as solid-state power supply units, oxygen membranes, membrane reactors for oxidizing hydrocarbons, thermoelectric devices, and gas and magnetic field sensors. Among the transition-metal oxides, the unique feature of cobaltites is a pronounced spin state tuning of magnetic, electronic, and transport properties, giving rise to giant magnetoresistance [3–5], insulator-metal transition [6], spin state crossover [7], unusual types of magnetic orders, etc. [8–10].

As is well known, due to the strong competition between the crystal-field splitting energy Δ_{cf} and the intra-atomic (Hund) exchange interaction J_{ex}, a Co^{3+} ion exhibits three alternative spin configurations: low-spin (LS, $S = 0$; $t_{2g}^6 e_g^0$), intermediate-spin (IS, $S = 1$; $t_{2g}^5 e_g^1$), and high-spin (HS, $S = 2$; $t_{2g}^4 e_g^2$) states [11]. The spin state of Co^{3+} ions can be switched by changes in the chemical doping level of an A and/or B sublattice, and by changing the synthesis conditions or external parameter, such as pressure [12–14], strain [15], or electric field [16].

The parent compound LaCoO$_3$ behaves up to 30 K very similar to a diamagnetic insulator with paramagnetic defects with Co^{3+} ions in a low-spin state [1]. In the interval $35 <$ $T < 110$ K, the fraction of IS Co^{3+} ions exponentially increases with temperature. The IS Co^{3+} is stabilized by a local dynamic Jahn-Teller deformation [17,18]. In the range $110 < T < 350$ K the population of IS/HS ions appears to stabilize near 50% as a result of the short-range ordering of LS and IS/HS cobalt [19]. At temperatures above 500 K, a gradual semiconductor-metal transition is observed with an increase in magnetization with increasing temperature. These transitions are accompanied by a sharp increase of the IS Co^{3+} ion fraction.

The preparation of oxygen-stoichiometric La$_{1-x}$Sr$_x$CoO$_3$ without high oxygen pressure is restricted to the compositional range $0 \leqslant x \leqslant 0.5$ [18]. The substitution of La^{3+} with Sr^{2+} ions leads to a drop of resistivity and the appearance of long-range ferromagnetic order above a 18% replacement of La^{3+} ions [20]. The highest Curie temperature ($T_C \sim 305$ K) is observed for stoichiometric metallic SrCo^{4+}O$_3$ [21]. It was shown that the basic compound SrCoO$_{3-\gamma}$ can have various structural distortions depending on the synthesis conditions and, as a consequence, on the oxygen content. SrCoO$_{3-\gamma}$ has an orthorhombic distortion at $\gamma = 0.5$, a tetragonal one at $\gamma \approx 0.15$, and in the case of close to stoichiometric in oxygen, the crystal structure is characterized by a cubic unit cell with the space group $Pm\overline{3}m$ [21]. A decrease in the oxygen content leads to the transition from the ferromagnetic state with $T_C \approx 305$ K ($\gamma \approx 0$) to the antiferromagnetic state with $T_N \approx 537$ K ($\gamma \approx 0.5$) [22]. The interaction between the variable spin state and the lattice is an additional source of phase separation in cobaltites. Thus, the coexistence of ferromagnetic and glassy states was observed in La$_{1-x}$Sr$_x$CoO$_3$ for various doping levels up to $x = 0.5$ [20,23,24]. Unlike

*Corresponding author: rommelfiz1@gmail.com

TABLE I. Crystal structural parameters, magnetic ordering temperature, and spontaneous magnetization values of the $La_{1-x}Sr_xCo_{1-y}Ni_yO_{3-\gamma}$ series of solid solutions.

Sample	Space group	a, b (Å)	c (Å)	V (Å³)	T_{mo} (K)	M_S (μ_B/f.u.)	$M_{S_{Co}}$ (μ_B/Co)
$La_{0.9}Sr_{0.1}Co_{0.95}Ni_{0.05}O_{2.88}$	$R\bar{3}c$	5.45(1)	13.14(3)	337.5(2)	87	0.44(3)	0.46(2)
$La_{0.9}Sr_{0.1}Co_{0.90}Ni_{0.10}O_{2.86}$	$R\bar{3}c$	5.45(2)	13.14(2)	337.9(2)	96	0.59(4)	0.66(2)
$La_{0.9}Sr_{0.1}Co_{0.85}Ni_{0.15}O_{2.82}$	$R\bar{3}c$	5.45(2)	13.14(2)	338.3(4)	120	0.77(2)	0.91(2)
$La_{0.9}Sr_{0.1}Co_{0.80}Ni_{0.20}O_{2.84}$	$R\bar{3}c$	5.45(3)	13.14(4)	338.5(2)	134	0.82(2)	1.03(5)
$La_{0.9}Sr_{0.1}Co_{0.75}Ni_{0.25}O_{2.85}$	$R\bar{3}c$	5.45(5)	13.15(3)	338.9(4)	141		
$La_{0.82}Sr_{0.18}Co_{0.95}Ni_{0.05}O_{2.845}$	$R\bar{3}c$	5.45(2)	13.17(2)	338.2(5)	173	1.12(2)	1.18(3)
$La_{0.82}Sr_{0.18}Co_{0.90}Ni_{0.10}O_{2.847}$	$R\bar{3}c$	5.45(4)	13.17(5)	338.2(5)	179	1.09(5)	1.21(4)
$La_{0.82}Sr_{0.18}Co_{0.80}Ni_{0.20}O_{2.781}$	$R\bar{3}c$	5.44(9)	13.17(4)	338.6(4)	168	1.06(3)	1.33(4)
$La_{0.7}Sr_{0.3}Co_{0.95}Ni_{0.05}O_{2.871}$	$R\bar{3}c$	5.44(3)	13.20(3)	338.7(2)	218	1.41(4)	1.49(4)
$La_{0.7}Sr_{0.3}Co_{0.90}Ni_{0.10}O_{2.826}$	$R\bar{3}c$	5.44(0)	13.19(2)	338.1(3)	209	1.34(3)	1.49(3)
$La_{0.7}Sr_{0.3}Co_{0.85}Ni_{0.15}O_{2.852}$	$R\bar{3}c$	5.44(0)	13.19(3)	338.0(3)	196	1.22(5)	1.43(4)
$La_{0.7}Sr_{0.3}Co_{0.80}Ni_{0.20}O_{2.786}$	$Pm\bar{3}m$	3.90(2)	3.90(2)	59.4(3)	191	1.13(5)	1.41(4)
$La_{0.5}Sr_{0.5}Co_{0.95}Ni_{0.05}O_{2.86}$	$Pm\bar{3}m$	3.83(1)	3.83(2)	56.2(3)	231	1.61(5)	1.69(3)
$La_{0.5}Sr_{0.5}Co_{0.90}Ni_{0.10}O_{2.76}$	$Pm\bar{3}m$	3.83(1)	3.83(2)	56.2(2)	211	1.46(3)	1.63(5)
$La_{0.5}Sr_{0.5}Co_{0.85}Ni_{0.15}O_{2.80}$	$Pm\bar{3}m$	3.83(2)	3.83(2)	56.2(2)	193	1.42(2)	1.67(3)
$La_{0.5}Sr_{0.5}Co_{0.84}Ni_{0.16}O_{2.82}$	$Pm\bar{3}m$	3.83(2)	3.83(2)	56.2(3)	184	1.41(5)	1.67(4)

the systems with a substitution in one (A or B) sublattice, the double-substituted cobaltites remain less explored. In this study, we explore the $La_{1-x}Sr_xCo_{1-y}Ni_yO_{3-\gamma}$ complex oxides by means of magnetization measurements, x-ray powder diffraction, and iodometric techniques. We provide an explanation of the mechanism by the change in the magnetic and transport properties upon the replacement of ions in both sublattices, accompanied by a change in the crystal structure.

II. EXPERIMENTAL DETAILS

Polycrystalline samples of solid solutions $La_{1-x}Sr_xCo_{1-y}Ni_yO_{3-\gamma}$ were prepared for Sr contents $x = 0.1, 0.18, 0.3, 0.5$ and Ni contents $0.05 \leqslant y \leqslant 0.25$ by a two-step solid state reaction method. The initial reagents La_2O_3, $SrCO_3$, Co_3O_4, and Ni_2O_3 of high purity were taken in the stoichiometric ratio and thoroughly mixed in a Retsch planetary ball mill for 30 min at a speed of 250 rpm. The preliminary synthesis was carried out for 21–22 h at a temperature of 1000 °C. Then obtained samples were ground again and a final synthesis was carried out at a temperature range 1200–1350 °C for about 5–9 h with cooling for at least 10 h down to a temperature of 300 °C. As the Ni content increased, the synthesis temperature also increased.

X-ray diffraction studies of the samples were performed using an x-ray diffractometer DRON-3M (Cu $K\alpha$ radiation) at room temperature. The scanning step was no more than 0.03°, and the exposure time was no less than 5 s. The data were recorded automatically. The spectra were processed using the FULLPROF software package [25].

Magnetic and magnetoresistive measurements were performed on a universal measuring device for physical properties (Cryogenic Ltd.) in magnetic fields up to 14 T and in the temperature range 5–315 K. Conductivity measurements were performed using a standard four-contact method with indium contacts deposited by ultrasound. The oxygen content was determined by iodometry.

III. RESULTS

A. X-ray diffraction

It was found that for La^{3+} substitution levels up to $x = 0.3$ the samples were single phase with different contents of Ni ions. For instance, in the subsystem $La_{0.5}Sr_{0.5}Co_{1-y}Ni_yO_{3-\gamma}$, a Co ion substitution level of more than 16% leads to the formation of a second impurity phase, different from the main one with a perovskite structure, whereas the $La_{0.9}Sr_{0.1}Co_{1-y}Ni_yO_{3-\gamma}$ subsystem is a single phase up to 25% of Ni ion content.

The results of the x-ray diffraction and chemical analysis are presented in Table I. It was found that in the $La_{1-x}Sr_xCo_{1-y}Ni_yO_{3-\gamma}$ system the unit cell is described in terms of the rhombohedral $R\bar{3}c$ space group for the $La_{0.9}Sr_{0.1}Co_{1-y}Ni_yO_{3-\gamma}$ subsystem and goes over to the cubic unit cell with the $Pm\bar{3}m$ space group for the $La_{0.5}Sr_{0.5}Co_{1-y}Ni_yO_{3-\gamma}$ subsystem. It is important to note that the $R\bar{3}c \rightarrow Pm\bar{3}m$ structural phase transition was observed in the $La_{0.7}Sr_{0.3}Co_{1-y}Ni_yO_{3-\gamma}$ subsystem with increasing Ni ion content. With an increase in the content of Ni ions, a change in the parameters of the unit cell should be expected, however, not observed, as with a change in the La^{3+}/Sr^{2+} ratio. This anomaly may indicate a spin crossover of Co^{3+} ions, which have different ionic radii in distinct spin states [1].

B. Iodometry

The determination of oxygen content by the iodometric titration method consists of several steps. First, the sample (20–60 mg) was dissolved in dilute hydrochloric acid containing KI (always kept above metallic Zn and never deposited into air). The following redox reactions take place:

$$2Co^{3+} + 3I^- \rightarrow 2Co^{2+} + I_3^-, \tag{1}$$

$$Co^{4+} + 3I^- \rightarrow Co^{2+} + I_3^-. \tag{2}$$
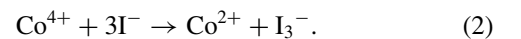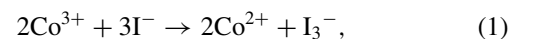
The released iodine was titrated with $Na_2S_2O_3$ and there the amount was determined by the following reaction:

$$I_3^- + 2S_2O_3^{2-} \rightarrow 3I^- + S_4O_6^{2-}. \qquad (3)$$
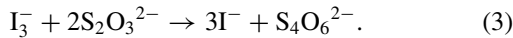
The titration endpoint was detected using a starch indicator. The oxidation state of Ni ions can be 2+ or 3+. According to the x-ray absorption spectroscopy data, at low Ni ion contents in manganites, the oxidation level of Ni ions is 2+ [26,27]. It was found that the 2+ oxidation state of Ni ions is more stable, and Ni^{3+} in a perovskite structure has poor thermal stability [28,29]. Further, based on the above facts, the oxidation state of Ni ions will be measured equal to 2+. Based on this assumption, the amount of released iodine is determined only by the average oxidative state of Co ions.

Iodometric studies have shown that Co ions are predominantly in the trivalent state for $La_{0.9}Sr_{0.1}Co_{1-y}Ni_yO_{3-\gamma}$ and $La_{0.82}Sr_{0.18}Co_{1-y}Ni_yO_{3-\gamma}$ subsystems with an insignificant fraction of Co^{2+} ions. Subsystems $La_{0.7}Sr_{0.3}Co_{1-y}Ni_yO_{3-\gamma}$ and $La_{0.5}Sr_{0.5}Co_{1-y}Ni_yO_{3-\gamma}$ are characterized by an increase in the average oxidation state of Co ions. With an increase in the replacement of La^{3+} ions by Sr^{2+} ions, the solubility limit of Ni^{2+} ions decreases and amounts to 16% for a subsystem with a 50% substitution of Sr^{2+} (Table I).

C. Magnetometry

Figures 1–4 show the isothermal magnetization hysteresis data (M-B) at 5 K in fields up to 14 T and temperature dependences of the magnetization (M-T) obtained on heating after cooling without a field [zero field cooled (ZFC)] and in a field of 0.02 T [field cooled (FC)] in the $La_{1-x}Sr_xCo_{1-y}Ni_yO_{3-\gamma}$ system. The substitution of Ni^{2+} ions for Co ions in the $La_{0.9}Sr_{0.1}Co_{1-y}Ni_yO_{3-\gamma}$ subsystem leads to an increase in the magnetization value and a simultaneous decrease in the coercive force value (Fig. 1). The magnetic transition is blurred across the field. With an increase in the content of Ni^{2+} ions the character of the field and temperature dependencees of the magnetization changes from those characteristic of a spin cluster glass to ones close to ferromagnetic. The magnetization is relatively high and there are no signs of saturation in fields of 14 T. This is a consequence of an increase in the fraction of ferromagnetically ordered clusters with an increase in the content of Ni^{2+} ions. The magnetic ordering temperature T_{mo} was obtained using the intersecting tangent method for the M vs T curves. An example is shown in Fig. 1(b). The magnetization value and magnetic ordering temperature T_{mo} rise with an increase in the Ni^{2+} content for the $La_{0.9}Sr_{0.1}Co_{1-y}Ni_yO_{3-\gamma}$ subsystem (Table I, Fig. 1). For the $La_{0.82}Sr_{0.18}Co_{1-y}Ni_yO_{3-\gamma}$ subsystem the character of the magnetization dependence is close to ferromagnetic even for low Ni^{2+} concentrations (Fig. 2). However, in the $La_{0.82}Sr_{0.18}Co_{1-y}Ni_yO_{3-\gamma}$ subsystem an increase in the Ni^{2+} content leads to a decrease of the magnetization value. T_{mo} is somewhat higher than in the $La_{0.9}Sr_{0.1}Co_{1-x}Ni_xO_{3-\gamma}$ subsystem and, with an increase in the content of Ni^{2+} ions, it first increases and then begins to decrease (Table I, Fig. 2). For $La_{0.7}Sr_{0.3}Co_{1-x}Ni_xO_{3-\gamma}$ and $La_{0.5}Sr_{0.5}Co_{1-x}Ni_xO_{3-\gamma}$ subsystems an increase in the portion of Ni^{2+} substituent ions entails a decrease in the magnetization and T_{mo} values (Figs. 3 and 4). The magnetic
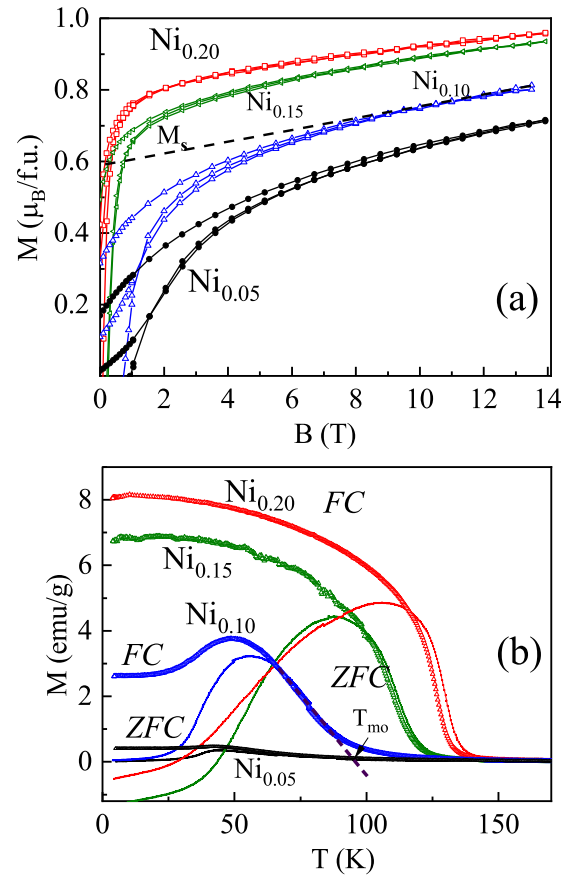

FIG. 1. Field [(a) $T = 5$ K] and temperature [(b) field cooling (FC) and zero field cooling (ZFC) measured at 0.02 T field] dependences of the magnetizations of the $La_{0.9}Sr_{0.1}Co_{1-y}Ni_yO_{3-\gamma}$ subsystem.

transition is somewhat blurred across the field. The field dependences of the magnetization are ferromagnetic, however, saturation in fields up to 14 T is not observed. The absence of saturation in fields up to 14 T for all samples may indicate the presence of some magnetic inhomogeneities. It is important to note that the maximum absolute values of magnetization were observed for the $La_{0.5}Sr_{0.5}Co_{1-x}Ni_xO_{3-\gamma}$ subsystem. At the same time, for this system, the substitution of Co ions by Ni^{2+} ions leads to a decrease in the magnetization values, as for the $La_{0.7}Sr_{0.3}Co_{1-x}Ni_xO_{3-\gamma}$ subsystem. In the $La_{0.9}Sr_{0.1}Co_{1-x}Ni_xO_{3-\gamma}$ subsystem, on the contrary, an increase in the concentration of Ni^{2+} ions leads to an increase in the magnetization values, which may indicate a gain of the ferromagnetic component fraction.

D. Transport properties

Figures 5 and 6 show the temperature dependences of the resistivity for the $La_{1-x}Sr_xCo_{1-y}Ni_yO_{3-\gamma}$ system. It can be seen that for a subsystem with a Sr^{2+} content of 10%, the temperature dependence of the resistivity has a semiconducting character, where the resistivity values at 5 K for samples with 10% and 15% Ni^{2+} content differ by several orders of magnitude. Thus, in this subsystem, an increase in the portion of Ni^{2+} ions leads to a sharp decrease in the resistivity values,
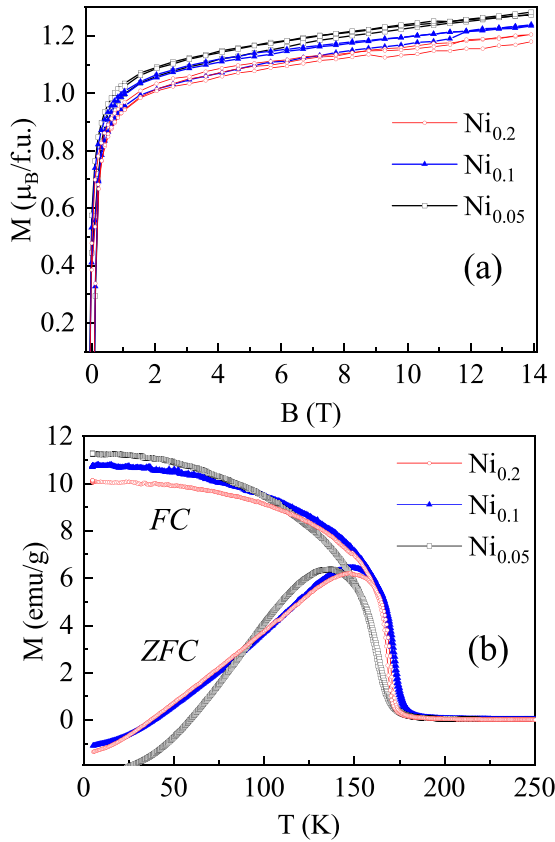
FIG. 2. Field [(a) $T = 5$ K] and temperature [(b) field cooling (FC) and zero field cooling (ZFC) measured at 0.02 T field] dependences of the magnetizations of the $La_{0.82}Sr_{0.18}Co_{1-y}Ni_yO_{3-\gamma}$ subsystem.

FIG. 3. Field [(a) $T = 5$ K] and temperature [(b) field cooling (FC) and zero field cooling (ZFC) measured at 0.02 T field] dependences of the magnetizations of the $La_{0.7}Sr_{0.3}Co_{1-y}Ni_yO_{3-\gamma}$ subsystem.

which is associated with the approach to the ferromagnetic cluster percolation threshold. Apparently, the substitution of Co ions by Ni^{2+} ions contributes to the stabilization of a part of the Co^{3+} ions in the IS state, similar to the replacement of La^{3+} by Sr^{2+}, which leads to an increase in the fraction of ferromagnetic conducting clusters with IS Co^{3+} ions and an observed sharp decrease in the resistivity values due to the approach to the percolation threshold of ferromagnetic clusters in the diamagnetic matrix of LS Co^{3+} ions. In the $La_{0.82}Sr_{0.18}Co_{1-y}Ni_yO_{3-\gamma}$ subsystem at room temperature, the dependence of the resistivity has a metallic character of conductivity. At a temperature of $\sim$180 K, an anomaly is observed, which coincides with the magnetic ordering temperature. The resistivity value sharply decreases and a minimum is observed at $\sim$135 K, after which the resistivity begins to increase and the nature of the dependence becomes close to that of a semiconductor. The presence of a minimum resistivity can be associated with the maximum concentration of Co^{3+} ions in the IS state [Fig. 6(a)]. Thus, it is assumed that as the temperature rises, some of the Co^{3+} ions pass from a LS to an IS state with a maximum IS Co^{3+} concentration near the resistivity minimum, and with a further increase in temperature, it undergoes a gradual transition to the mixed IS/HS state with a decrease in the fraction of IS Co^{3+} ions, which is expressed in an increased resistivity of the samples.

The spin states of the Co^{3+} matrix change with temperature very similarly to $LaCoO_3$ [1,17–19].

A further replacement of La^{3+} ions by Sr^{2+} ions and Co ions by Ni^{2+} ions leads to an increase in the fraction of the conducting phase and a change in the character of conductivity to metallic [Fig. 6(b)]. At temperatures that coincide with the temperature of magnetic ordering for the subsystems with $x = 0.3$ and 0.5, as well as for the subsystem with $x = 0.18$, similar anomalies are observed [marked with an asterisk, Fig. 6(b)]. In addition, at temperatures close to helium, an insignificant increase in the resistivity values of the samples is observed.

IV. DISCUSSION

According to the semiempirical rules of Goodenough-Kanamori [22], strong antiferromagnetic exchange interactions in this system will be interactions of the type $Co^{3+}(HS)$-O^{2-}-$Co^{3+}(HS)$, Ni^{2+}-O^{2-}-Ni^{2+}, Ni^{2+}-O^{2-}-$Co^{3+}(HS)$, $Co^{2+}(HS)$-O^{2-}-$Co^{3+}(HS)$, and $Co^{2+}(HS)$-O^{2-}-$Co^{2+}(HS)$. LS Co^{3+} ions will not interact with other ions of the B sublattice. The interactions of Co^{4+}-O^{2-}-$Co^{3+}(HS)$ ions are weakly ferromagnetic, Ni^{2+}-O^{2-}-Co^{4+} moderately
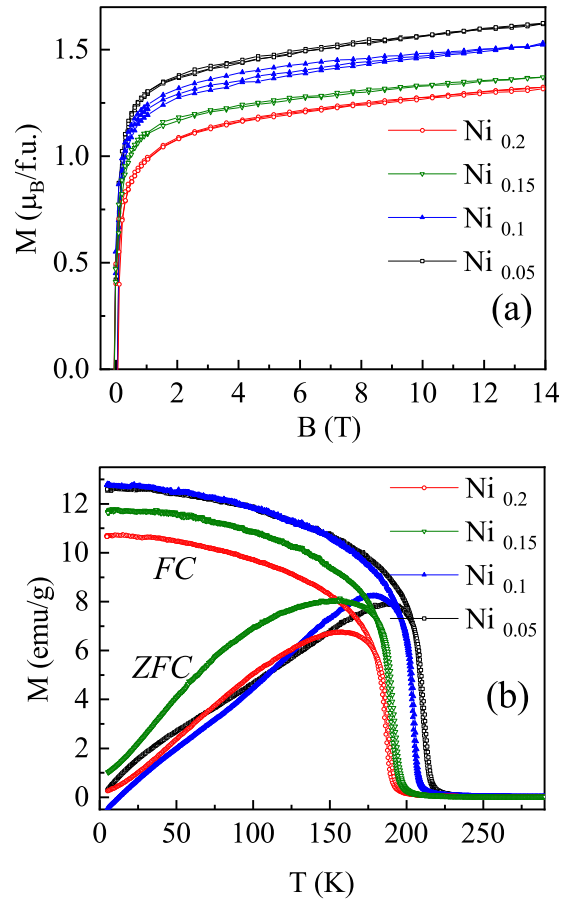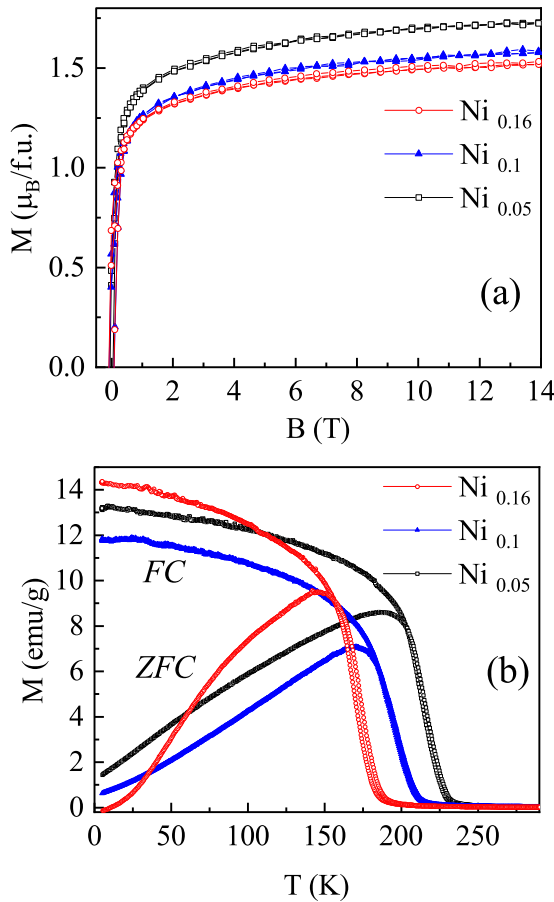
FIG. 4. Field [(a) $T = 5$ K] and temperature [(b) field cooling (FC) and zero field cooling (ZFC) measured at 0.02 T field] dependences of the magnetizations of the $La_{0.5}Sr_{0.5}Co_{1-y}Ni_yO_{3-\gamma}$ subsystem.

FIG. 5. Temperature dependences of the resistivity for the $La_{0.9}Sr_{0.1}Co_{1-y}Ni_yO_{3-\gamma}$ subsystem.

ferromagnetic, and the interactions of Co^{3+}(IS) ions with each other are ferromagnetic [7,30–32].

When considering the $La_{1-x}Sr_xCoO_3$ system by Goodenough, Zhow, and Yamaguchi *et al.* [17,18], the theory was given that then La^{3+} ions are replaced by Sr^{2+} ions, the strong covalent bonding of the $Co^{4+}O_6$ LS complex stabilizes IS Co^{3+} at the nearest-neighbor cobalt, and a ferromagnetic electron transfer from IS Co^{3+} to LS Co^{4+} gives rise to superparamagnetic clusters below T_C of the cluster. The spin states of the Co^{3+} matrix change with temperature in a similar way, as in $LaCoO_3$. For $0.05 \leqslant x \leqslant 0.15$, the superparamagnetic clusters interact through the Co^{3+} matrix to form a spin glass, and for $x \geqslant 0.2$ the ferromagnetic clusters percolate through the matrix to give long-range ferromagnetic ordering below T_C, and purely metallic behavior was observed only for $x \geqslant 0.3$.

In the considered anion-deficient system $La_{1-x}Sr_xCo_{1-y}Ni_yO_{3-\gamma}$, the Co^{4+} ions were detected for Sr^{2+} concentrations $x = 0.5$ and 0.3 according to the data of the iodometric analysis. In the $La_{0.7}Sr_{0.3}Co_{1-y}Ni_yO_{3-\gamma}$ subsystem its fraction of the total number of Co^{4+} ions does not exceed 9.7%. Thus, the implementation of the IS Co^{3+} stabilization mechanism proposed by Goodenough *et al.* [17,18] can be realized only in the $La_{0.5}Sr_{0.5}Co_{1-y}Ni_yO_{3-\gamma}$ subsystem.
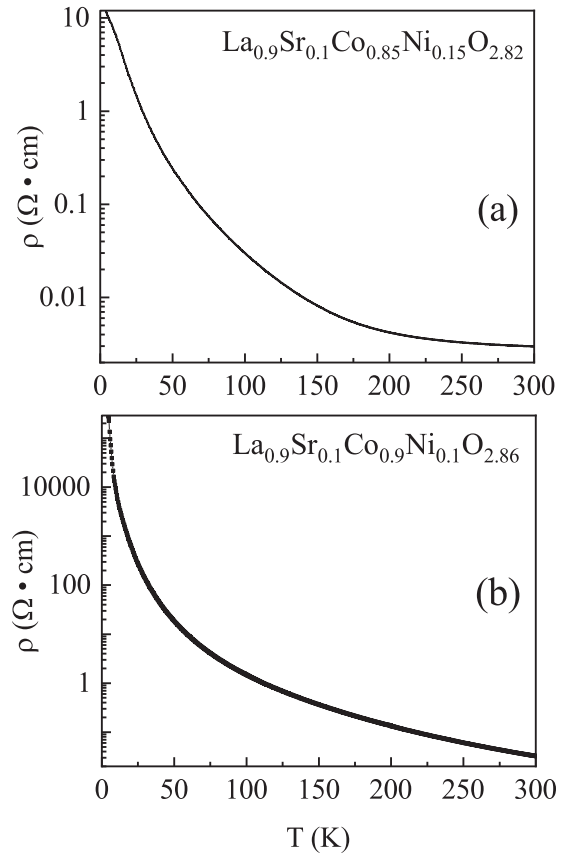
In the anion-deficient $La_{1-x}Sr_xCo_{1-y}Ni_yO_{3-\gamma}$ system, a complex competition of exchange interactions of different signs between ions in the B sublattice is realized, and the system can be divided into several concentration regions. We assume that the replacement of La^{3+} ions by Sr^{2+} ions in the $La_{1-x}Sr_xCo_{1-y}Ni_yO_{3-\gamma}$ system leads to an increase in the Co^{3+}-O bond lengths in the CoO_6 octahedra, which entails the stabilization of Co^{3+} ions in the IS state. In this case, ferromagnetism would be caused by vibronic superexchange interactions between octahedral IS Co^{3+} ions in the presence of dynamic Jahn-Teller distortions. This assumption is in good agreement with the one in Ref. [31] supporting ferromagnetically interacting IS Co^{3+} ions, in which Nb^{5+} ions were simultaneously introduced into the B sublattice to prevent the appearance of Co^{4+} ions. In Ref. [31] it was also shown that long-range ferromagnetic order does not arise owing to diamagnetic dilution by Nb ions. In the anion-deficient $La_{1-x}Sr_xCo_{1-y}Ni_yO_{3-\gamma}$ system an "analog" of dilution with Nb^{5+} ions in the $La_{1-x}Sr_xCo_{1-x/2}Nb_{x/2}O_3$ system is diluted with antiferromagnetically interacting Ni^{2+} ions. At the same time, the presence of oxygen vacancies leads to the stabilization of Co^{3+} ions in the HS (CoO_5 oxygen pyramids) [33]. This causes the magnetic inhomogeneity of the compounds under consideration. The absence of saturation of the magnetization in fields up to 14 T may indicate a competition between ferromagnetic and antiferromagnetic exchange interactions. This mechanism is most clearly manifested in subsystems
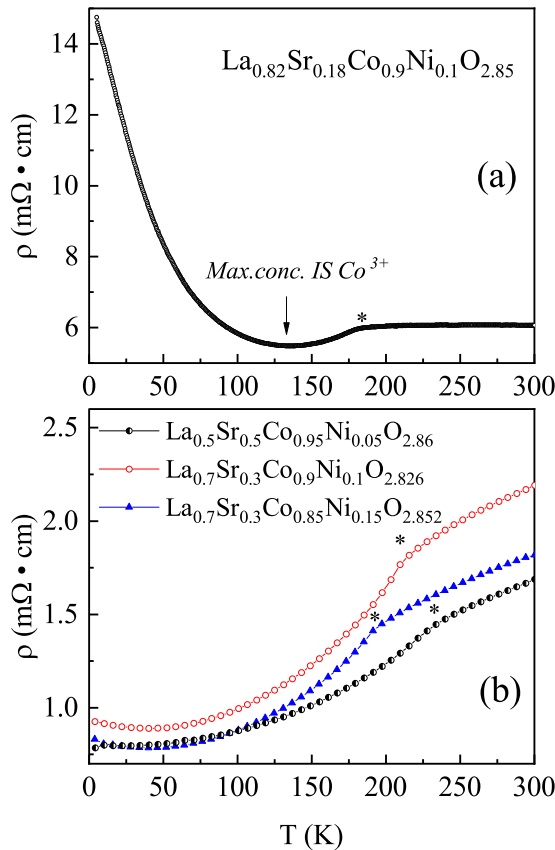
FIG. 6. Resistivity temperature dependences of various compositions. Anomalies correspond to the T_{mo} and are marked with an asterisk.

with a low level of substitution with Sr^{2+}. Also, it was established that oxygen deficiency leads to the destruction of the long-range ferromagnetic order characteristic for the stoichiometric $La_{0.5}Sr_{0.5}CoO_3$ compound [34], that is in common with our model.

For a subsystem with $x = 0.1$ the state of a cluster spin glass with a semiconducting character of the resistivity dependence is realized. With an increase in the substitution of Co^{3+} ions by Ni^{2+} ones, the fraction of the ferromagnetic conducting phase gradually increases, due to the stabilization of IS Co^{3+} ions in CoO_6 octahedra and approaching the percolation threshold of ferromagnetic clusters in the diamagnetic LS Co^{3+} matrix. The transition to the magnetic phase is strongly spread over the field, which indicates a strong magnetic inhomogeneity and the absence of long-range magnetic ordering. Anomalies in the dependences of magnetization at 5% and 10% Ni^{2+} substitution at low temperatures can be explained by the thermally induced spin crossover of a part of Co^{3+} ions, first from the LS to the IS state, and then to the mixed IS/HS state. With an increase in the Sr substitutional levels, the fraction of the ferromagnetic conducting phase and T_{mo} values grow as well. Simultaneously, the degree of rhombohedral distortions is reduced, followed by the $R\bar{3}c \rightarrow Pm\bar{3}m$ structural phase transition.

In the subsystem with $x = 0.18$, the case of a metallic dependence of the conductivity in the paramagnetic region with

a transition to a mixed type of conductivity in the magnetically ordered region and a minimum of absolute values in the region of ~130 K is realized. With an increase in the concentration of Ni^{2+} ions, as in the $La_{0.9}Sr_{0.1}Co_{1-y}Ni_yO_{3-\gamma}$ subsystem, the IS Co^{3+} ion is stabilized; however, the absolute values of the magnetization begin to decrease due to an increase in the fraction of antiferromagnetic inclusions due to doping with Ni^{2+} ions. T_{mo} initially increases with a rise in the Ni^{2+} concentration, and then begins to decrease.

In the $La_{0.7}Sr_{0.3}Co_{1-y}Ni_yO_{3-\gamma}$ and $La_{0.5}Sr_{0.5}Co_{1-y}Ni_yO_{3-\gamma}$ subsystems, the same anomalies in the resistivity dependences are observed, which coincide with the temperature of magnetic ordering, as in the $La_{0.82}Sr_{0.18}Co_{1-y}Ni_yO_{3-\gamma}$ subsystem, however, such a clearly pronounced resistivity minimum is no longer observed and the resistivity is predominantly metallic in nature in all regions. An increase in the portion of Ni^{2+} ions leads to a decrease in the T_{mo} and magnetization values for both $x = 0.3$ and $x = 0.5$ subsystems, which indicates the dilution of the ferromagnetic matrix with antiferromagnetic inclusions due to an increase in the concentration of Ni^{2+} ions, the exchange interactions of which in the considered anion-deficient systems are predominantly antiferromagnetic. The stabilizing effect of IS Co^{3+} with an increase in the Ni^{2+} concentration already makes a smaller contribution than the effect of a decrease in the fraction of Co ions in the B sublattice. In addition, these subsystems can implement the mechanism of stabilization of IS Co^{3+} ions at the nearest-neighborhood of Co^{4+} ions proposed by Goodenough *et al.* [17,18].

Despite the absence of saturation of magnetization in fields up to 14 T, it is possible to approximately estimate the values of spontaneous magnetization in order to estimate the fraction of ferromagnetically interacting ions of the B sublattice. As mentioned earlier, in the system under consideration, these will be mainly IS Co^{3+} ions. The results of the spontaneous magnetization calculations in μ_B/f.u. (M_S) and in μ_B/Co ($M_{S_{Co}}$) are given in Table I. It is well seen that for the $x = 0.1$ subsystem with an increase in the portion of Ni^{2+} ions an increase in both the M_S values and the $M_{S_{Co}}$ values is observed. For $x = 0.18$ the growth of M_S values with an increase of Ni^{2+} stops and for $x = 0.3$ and 0.5 the M_S values begin to decrease. According to our model, this is a consequence of the predominance of the effect of dilution with nickel ions for subsystems strongly substituted by Sr^{2+}. At the same time, for the $x = 0.3$ and $x = 0.5$ subsystems the $M_{S_{Co}}$ values stabilize.

V. CONCLUSION

Our study shows the double-substitution results in pronounced changes in the structural, magnetic, and transport properties of the anion-deficient $La_{1-x}Sr_xCo_{1-y}Ni_yO_{3-\gamma}$ system. Surely, this system cannot by described only in terms of HS or IS Co^{3+}. With the replacement of La^{3+} ions by Sr^{2+} ions the stabilization of Co^{3+} ions in the IS state (LS to IS transition) occurs. In this case, ferromagnetism would be caused by vibronic superexchange interactions between octahedral IS Co^{3+} ions in the presence of dynamic Jahn-Teller distortions. For low levels of Sr and Ni ion substitution, the system demonstrates cluster spin-glass behavior with a semiconducting character of the resistivity dependence and a

diamagnetic LS Co^{3+} matrix. Substitution by Ni ions leads to the stabilization of IS Co^{3+} ions in CoO_6 octahedra, approaching the percolation threshold of ferromagnetic clusters in the diamagnetic matrix. Also, the thermally induced spin crossover of part of the Co^{3+} ions, first from the LS to the IS state, and then to the mixed IS/HS state, takes place.

The increase in the Sr substitutional levels results in the reduction of the degree of rhombohedral distortions and the $R\bar{3}c \rightarrow Pm\bar{3}m$ structural phase transition. This process is accompanied by a gradual change in the nature of the dependence of conductivity from a semiconductor to that for metals through intermediate compositions with a mixed type of conductivity. For high levels of substitution with Sr ions, the substitution with Ni ions in the B sublattice leads only to dilution by antiferromagnetically interacting Ni ions, which leads to a decrease in the magnetization values. Since in the system under consideration the ferromagnetically interacting ions are mainly IS Co^{3+} and $M_{S_{Co}}$ values are not sensitive to Ni ion substitution for high Sr replaced subsystems, we assume that the effect of stabilization of IS Co^{3+}, as for low levels of Sr ion substitution subsystems, is not present or negligible in comparing with the effect of dilution by antiferromagnetically interacting Ni ions. For strongly Sr-substituted subsystems the mechanism of the stabilization of IS Co^{3+} ions at the nearest neighbor of Co^{4+} ions proposed by Goodenough *et al.* [17,18] can also be implemented. Long-range ferromagnetic order does not arise owing to dilution by antiferromagnetic Ni ions and due to the presence of oxygen vacancies leading to long-range ferromagnetic order destruction [33,34].

[1] N. B. Ivanova, S. G. Ovchinnikov, M. M. Korshunov, I. M. Eremin, and N. V. Kazak, Phys. Usp. **52**, 789 (2009).

[2] B. Raveau and M. Seikh, *Cobalt Oxides: From Crystal Chemistry to Physics* (Wiley, Hoboken, NJ, 2012).

[3] A. Maignan, C. Martin, D. Pelloquin, N. Nguyen, and B. Raveau, J. Solid State Chem. **142**, 247 (1999).

[4] I. O. Troyanchuk, N. V. Kasper, D. D. Khalyavin, H. Szymczak, R. Szymczak, and M. Baran, Phys. Rev. Lett. **80**, 3380 (1998).

[5] I. O. Troyanchuk, M. V. Bushinsky, A. V. Nikitin, L. S. Lobanovsky, A. M. Balagurov, V. Sikolenko, V. Efimov, and D. V. Sheptyakov, J. Appl. Phys. **113**, 053909 (2013).

[6] C. Frontera, J. L. García-Muñoz, A. Llobet, and M. A. G. Aranda, Phys. Rev. B **65**, 180405(R) (2002).

[7] Y. Okimoto, T. Saitoh, Y. Kobayashi, and S. Ishihara, *Spin-Crossover Cobaltite: Review and Outlook*, Vol. 305 (Springer, Berlin, 2021).

[8] I. O. Troyanchuk, D. V. Karpinsky, A. P. Sazonov, V. Sikolenko, V. Efimov, and A. Senyshyn, J. Mater. Sci. **44**, 5900 (2009).

[9] I. O. Troyanchuk, M. V. Bushinsky, N. V. Tereshko, R. A. Lanovsky, V. V. Sikolenko, C. Ritter, Y. S. Orlov, and S. G. Ovchinnikov, Mater. Res. Express **6**, 026105 (2018).

[10] D. D. Khalyavin, D. N. Argyriou, U. Amann, A. A. Yaremchenko, and V. V. Kharton, Phys. Rev. B **75**, 134407 (2007).

[11] M. A. Korotin, S. Y. Ezhov, I. V. Solovyev, V. I. Anisimov, D. I. Khomskii, and G. A. Sawatzky, Phys. Rev. B **54**, 5309 (1996).

[12] T. Vogt, J. A. Hriljac, N. C. Hyatt, and P. Woodward, Phys. Rev. B **67**, 140401(R) (2003).

[13] J.-S. Zhou, J.-Q. Yan, and J. B. Goodenough, Phys. Rev. B **71**, 220103(R) (2005).

[14] I. Fita, R. Szymczak, R. Puzniak, I. O. Troyanchuk, J. Fink-Finowicki, Y. M. Mukovskii, V. N. Varyukhin, and H. Szymczak, Phys. Rev. B **71**, 214404 (2005).

[15] D. Fuchs, C. Pinta, T. Schwarz, P. Schweiss, P. Nagel, S. Schuppler, R. Schneider, M. Merz, G. Roth, and H. v. Löhneysen, Phys. Rev. B **75**, 144402 (2007).

[16] A. Herklotz, A. D. Rata, L. Schultz, and K. Dörr, Phys. Rev. B **79**, 092409 (2009).

[17] S. Yamaguchi, Y. Okimoto, and Y. Tokura, Phys. Rev. B **55**, R8666 (1997).

[18] S. L. Cooper, T. Egami, J. B. Goodenough, and J.-S. Zhou, *Localized to Itinerant Electronic Transition in Perovskite Oxides*, Vol. 98 (Springer, Berlin, 2003).

[19] P. M. Raccah and J. B. Goodenough, Phys. Rev. **155**, 932 (1967).

[20] J. Wu and C. Leighton, Phys. Rev. B **67**, 174408 (2003).

[21] Y. Long, Y. Kaneko, S. Ishiwata, Y. Taguchi, and Y. Tokura, J. Phys.: Condens. Matter **23**, 245601 (2011).

[22] A. Muñoz, C. delaCalle, J. A. Alonso, P. M. Botta, V. Pardo, D. Baldomir, and J. Rivas, Phys. Rev. B **78**, 054404 (2008).

[23] M. Itoh, I. Natori, S. Kubota, and K. Motoya, J. Phys. Soc. Jpn. **63**, 1486 (1994).

[24] D. N. H. Nam, K. Jonason, P. Nordblad, N. V. Khiem, and N. X. Phuc, Phys. Rev. B **59**, 4189 (1999).

[25] T. Roisnel and J. Rodríguez-Carvajal, Mater. Sci. Forum **378–381**, 118 (2001).

[26] O. Toulemonde, F. Studer, A. Barnabé, A. Maignan, C. Martin, and B. Raveau, Eur. Phys. J. B **4**, 159 (1998).

[27] O. Toulemonde, F. Studer, and B. Raveau, Solid State Commun. **118**, 107 (2001).

[28] G. Blasse, J. Phys. Chem. Solids **26**, 1969 (1965).

[29] K. Huang, H. Y. Lee, and J. B. Goodenough, J. Electrochem. Soc. **145**, 3220 (1998).

[30] M. R. Ibarra, R. Mahendiran, C. Marquina, B. García-Landa, and J. Blasco, Phys. Rev. B **57**, R3217 (1998).

[31] I. O. Troyanchuk, D. V. Karpinsky, and R. Szymczak, Phys. Status Solidi B **242**, R49 (2005).

[32] D. Phelan, D. Louca, S. Rosenkranz, S.-H. Lee, Y. Qiu, P. J. Chupas, R. Osborn, H. Zheng, J. F. Mitchell, J. R. D. Copley, J. L. Sarrao, and Y. Moritomo, Phys. Rev. Lett. **96**, 027201 (2006).

[33] D. V. Karpinsky, I. O. Troyanchuk, L. S. Lobanovsky, A. N. Chobot, C. Ritter, V. Efimov, V. Sikolenko, and A. L. Kholkin, J. Phys.: Condens. Matter **25**, 316004 (2013).

[34] R. P. Haggerty and R. Seshadri, J. Phys.: Condens. Matter **16**, 6477 (2004).